Available online at www.sciencedirect.com
ScienceDirect
Journal of Power Sources 178 (2008) 801–806
JOURNAL OF POWER SOURCES
www.elsevier.com/locate/jpowsour

Short communication

A study on the electrochemical characteristics of $LiFePO_4$ cathode for lithium polymer batteries by hydrothermal method

En Mei Jin [a], Bo Jin [a,b], Dae-Kyoo Jun [a], Kyung-Hee Park [a], Hal-Bon Gu [a,*], Ki-Won Kim [c]

[a] *Department of Electrical Engineering, Chonnam National University, Gwangju 500-757, South Korea*
[b] *College of Materials Science and Engineering, Jilin University, 130025 Changchun, China*
[c] *ITRC for Energy Storage and Conversion, Gyeongsang National University, 660-701 Jinju, South Korea*

Received 14 July 2007; received in revised form 11 September 2007; accepted 24 September 2007
Available online 29 September 2007

Abstract

Phospho-olivine $LiFePO_4$ cathode materials were prepared by hydrothermal reaction at 150 °C. Carbon black was added to enhance the electrical conductivity of $LiFePO_4$. $LiFePO_4$-C powders (0, 3, 5 and 10 wt.%) were characterized by X-ray diffraction (XRD) and transmission electron microscope (TEM). $LiFePO_4$-C/solid polymer electrolyte (SPE)/Li cells were characterized electrochemically by charge/discharge experiments at a constant current density of 0.1 mA cm^{-2} in a range between 2.5 and 4.3 V vs. Li/Li^+, cyclic voltammetry (CV) and ac impedance spectroscopy. The results showed that initial discharge capacity of $LiFePO_4$ was 104 mAh g^{-1}. The discharge capacity of $LiFePO_4$-C/SPE/Li cell with 5 wt.% carbon black was 128 mAh g^{-1} at the first cycle and 127 mAh g^{-1} after 30 cycles, respectively. It was demonstrated that cycling performance of $LiFePO_4$-C/SPE/Li cells was better than that of $LiFePO_4$/SPE/Li cells.

Keywords: $LiFePO_4$; Carbon black; Hydrothermal method; Solid polymer electrolyte

1. Introduction

Lithium polymer batteries are widely used in potential power sources for portable electronic devices such as cellular telephones, lap-top computers and cameras. The successful commercialization of Li-ion gel polymer batteries for portable electronic devices has led to other applications where the size and weight of batteries are important. A considerable investment in this battery technology that utilizes $LiCoO_2$ cathodes has been made [1–3]. However, low-cost cathode materials are required for many applications such as in electrical vehicles (EVs) and hybrid electric vehicles (HEVs) [4,5].

Recently, phosphates $LiMPO_4$ (M = Co, Mn, Fe and Ni) cathode materials, which provide high potentials and good reversible capacities over 150 mAh g^{-1} in practical uses [6]. Among this series of materials, $LiFePO_4$ is a low-cost material and highly compatible to the environment. $LiFePO_4$ has a highly stable three-dimensional framework due to strong P–O covalent bonds in $(PO_4)^{3-}$ polyanion, which prohibits the liberation of oxygen [7–10]. These characteristics provide an excellent safety under abuse conditions of the batteries. Phospho-olivine $LiFePO_4$ have been intensively investigated because of its high stability, low cost, high compatibility with environment [11,12]. However, it is difficult to attain its full capacity because its electronic conductivity is very low, and diffusion of Li^+ ion in the olivine structure is slow. The two ways of electronic conductive carbon coating and particle size reduction have been used to improve electronic conductivity of $LiFePO_4$ [13–16]. Various synthetic methods such as solid-state reaction, sol–gel route, hydrothermal reaction, co-precipitation method have been successfully used for these strategies and the synthesis of single-phase $LiFePO_4$ [17–20].

In this paper, phosphor-olivine $LiFePO_4$ cathode material was prepared by hydrothermal reaction. In order to enhance the electrical conductivity of $LiFePO_4$, carbon black was added after hydrothermal reaction. 25PVDF-$LiClO_4$EC$_{10}$PC$_{10}$ as polymer

* Corresponding author. Tel.: +82 62 530 0740; fax: +82 62 530 0077.
E-mail address: hbgu@chonnam.ac.kr (H.-B. Gu).

0378-7753/$ – see front matter © 2007 Elsevier B.V. All rights reserved.
doi:10.1016/j.jpowsour.2007.09.073

electrolyte which was reported previously by us was employed [21]. The electrochemical properties of $LiFePO_4$-C/solid polymer electrolyte (SPE)/Li coin-type cells were evaluated by cyclic voltammetry (CV), charge/discharge experiments and ac impedance spectroscopy.

2. Experimental

$LiFePO_4$ was prepared with the starting materials of $LiOH{\cdot}H_2O$ (Aldrich Co. 99.95%), $FeSO_4{\cdot}7H_2O$ (Aldrich Co. >99%), H_3PO_4 (Aldrich Co. >99.999%) and ascorbic acid (Aldrich Co. >99%). After $LiOH{\cdot}H_2O$ was dissolved in distilled water to obtain 1 M solution, H_3PO_4 and $FeSO_4{\cdot}7H_2O$ powders were added to LiOH solution in a molar ratio for Li:Fe:P = 3:1:1. A Telflon obturation vessel (TAF-SR-50, TAIATSU TECHNO) filled with the mixture was sealed in a stainless steel autoclave and heated at 150 °C for 3 h. After being cooled to room temperature, the solution was filtered to separate the precipitate powders; the powder was washed with ultra pure water. The obtained powder was dried at 100 °C for 1 h under vacuum. In order to improve low electronic conductivity of $LiFePO_4$, carbon black (3, 5 and 10 wt.%) was added into the solution of *N*-methylpyrrolidone (NMP) and $LiFePO_4$, the mixture was ball-milled for 10 h. After that, the mixture was dried at 90 °C for 12 h. The obtained powders were further dried at 400 °C for 1 h in nitrogen atmosphere. After being cooled to room temperature, the mixture of NMP and $LiFePO_4$-C was again ball-milled for 10 h. At last, the mixture was dried at 90 °C for 12 h.

Crystalline phases were identified with X-ray diffraction (XRD, Dmax/1200, Rigaku). XRD patterns were collected by a step-scanning mode in the range of 10–80° with a step time of $5^\circ\,min^{-1}$. Powder morphologies were observed by transmission electron microscope (TEM, JEOL JFE-2000 FXII).

Cathodes were made from mixtures of $LiFePO_4$-C powders, carbon black (SP270) and polyvinylidene fluoride (PVDF) binder dissolved in NMP in a weight ratio of 70:25:5. The obtained slurry was ball-milled for 1 h, and coated onto an Al-foil. The resulting electrode films were pressed with a twin roller, cut into a round plate ($\Phi = 15.958$ mm) and dried at 110 °C for 24 h under vacuum. 25PVDF-$LiClO_4EC_{10}PC_{10}$ as SPE was prepared by mixing of $LiClO_4$, propylene carbonate and ethylene carbonate in a mole ratio of 1:10:10, and finally polyvinylidenefluoride-hexafluoro propylene (Kynar 2801) was added.

$LiFePO_4$/SPE/Li and $LiFePO_4$-C/SPE/Li coin-type cells (CR2032) were assembled with lithium metal as anode and 25PVDF-$LiClO_4EC_{10}PC_{10}$ as SPE in an argon-filled glove box. CV testing was performed using WBCS3000 (WonATech Co.) battery tester system in a potential range of 2.3–4.5 V at a scanning rate of $0.1\,mV\,s^{-1}$. The test batteries were cycled galvanostatically in a potential range of 2.5–4.3 V using a WBCS3000 (WonATech Co.) battery tester system at a constant current density of $0.1\,mA\,cm^{-2}$.

Electrochemical impedance measurements were performed using an IM6 impedance system (Zahner Elektrik Company). The spectrum was potentiostatically measured by applying an ac voltage of 10 mV over the frequency range from 2 MHz to 10 mHz.

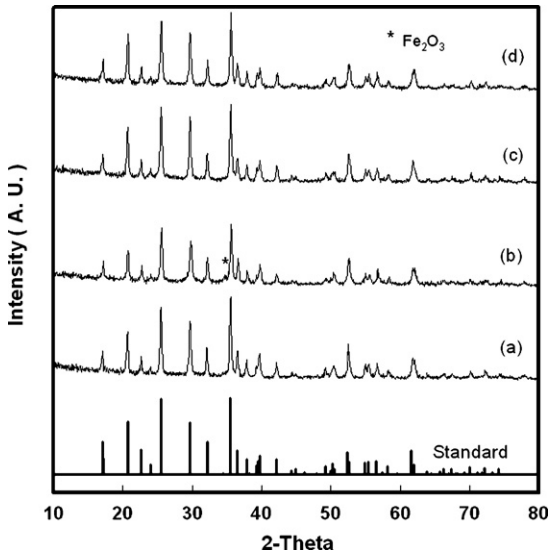

Fig. 1. XRD patterns for $LiFePO_4$-C powders with different carbon black contents (a) 0 wt.%, (b) 3 wt.%, (c) 5 wt.% and (d) 10 wt.%.

3. Results and discussion

3.1. XRD analysis of $LiFePO_4$-C powders

XRD patterns of $LiFePO_4$-C powders with different carbon black contents (0, 3, 5 and 10 wt.%) are shown in Fig. 1. All the patterns can be indexed to a single-phase material having an orthorhombic olivine-type structure (space group *Pmnb*), which are the same as the standard value (JCPDS card number: 40-1499). Impurity Fe_2O_3 is found only in $LiFePO_4$-C powders with 3 wt.% carbon black. Furthermore, the increasing peak intensity of $LiFePO_4$-C with 5 wt.% carbon black shows that particles with higher crystallinity are obtained. Also, the relative peak intensities change slightly with increasing carbon black content; therefore, there is apparently little change in morphology with increasing carbon black content. Lattice parameters of $LiFePO_4$-C powders with different carbon black contents (0, 3, 5 and 10 wt.%) are shown in Table 1. On increasing the carbon black content, the lattice parameters '*b*' and '*c*' are slightly decreased while the lattice parameter '*a*' is slightly increased.

Table 1
Lattice parameters of $LiFePO_4$-C powders (space group: *Pmnb*) with different carbon black contents

	Carbon black content			
	0 wt.%	3 wt.%	5 wt.%	10 wt.%
Cell constants				
a (Å)	5.9854	5.9944	6.0160	6.0015
b (Å)	10.4006	10.3104	10.4006	10.3404
c (Å)	4.7103	4.7053	4.7103	4.7024
V (Å^3)	293.22	290.81	294.72	291.82

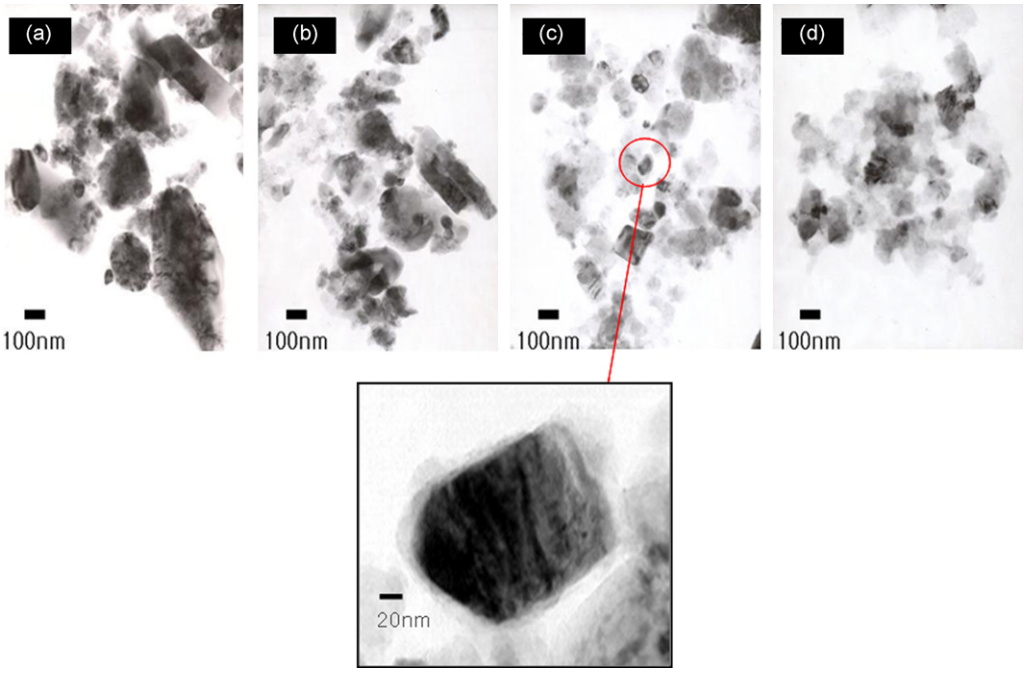

Fig. 2. TEM images of $LiFePO_4$-C powders with different carbon black contents (a) 0 wt.%, (b) 3 wt.%, (c) 5 wt.% and (d) 10 wt.%.

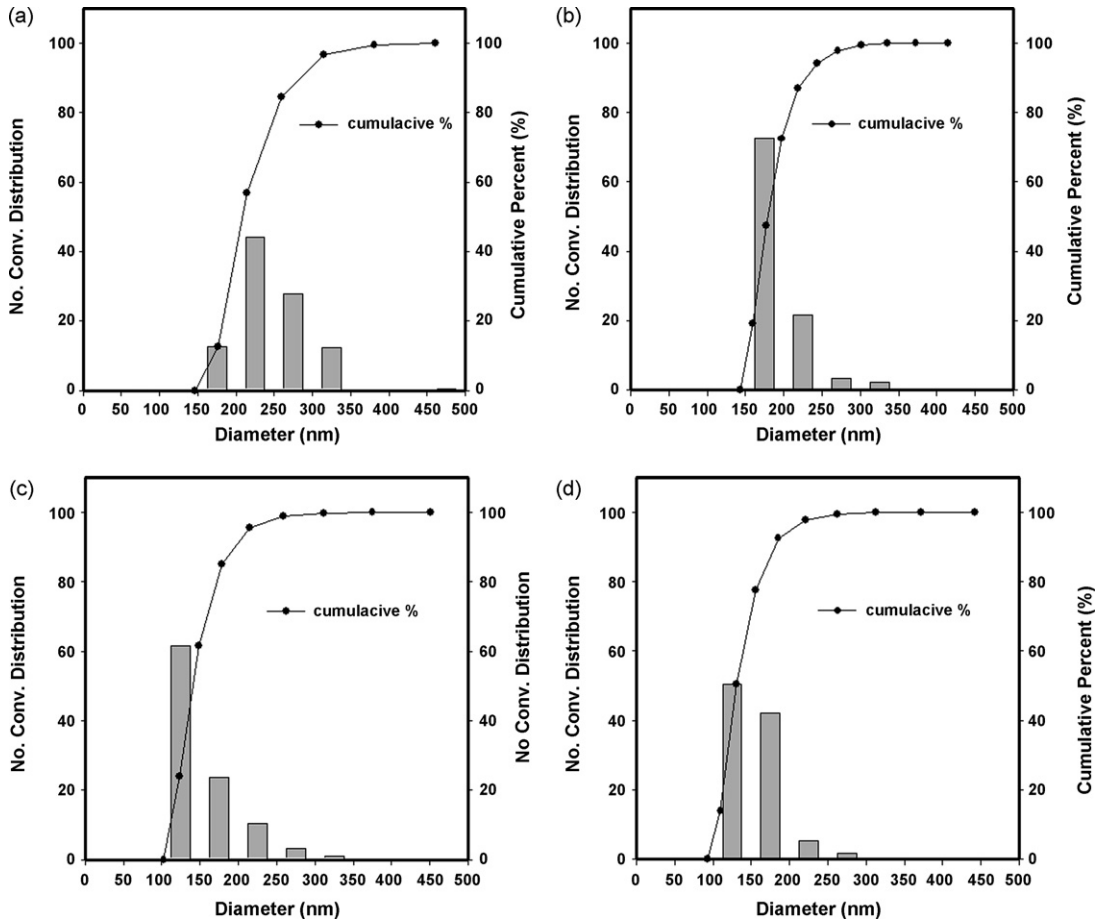

Fig. 3. Particle size distribution of LiFePO4-C powders with different carbon black contents (a) 0 wt.%, (b) 3 wt.%, (c) 5 wt.% and (d) 10 wt.%.

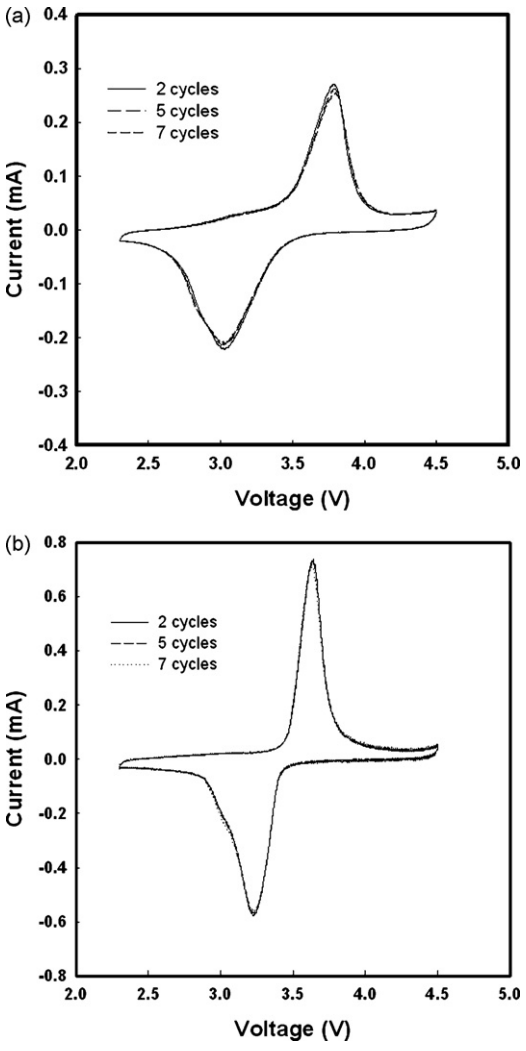

Fig. 4. Cyclic voltammograms of $LiFePO_4$-C/SPE/Li cells with different carbon black contents (a) 0 wt.% and (b) 5 wt.% at a scan rate of 0.1 mV s^{-1}.

It is demonstrated that the added carbon black does not change crystal structure of $LiFePO_4$.

3.2. TEM analysis of $LiFePO_4$-C powders

TEM images of $LiFePO_4$-C powders with different carbon black contents (0, 3, 5 and 10 wt.%) are shown in Fig. 2. As can be seen from Fig. 2, the particle size of $LiFePO_4$-C with 0, 3, 5 and 10 wt.% ranges from 200 to 300, 150 to 250, 100 to 200 and 100 to 200 nm, respectively. It is obvious that the particle size of $LiFePO_4$-C (3, 5 and 10 wt.%) powders is smaller than that of $LiFePO_4$ powders. The particles become more uniform and round in shape with increasing carbon black content. This demonstrates that carbon black in the mixture retards the particle growth during calcination. $LiFePO_4$-C particles agglomerate and form the secondary particles. The smaller particles, which shorten the lithium ions diffusion distances between the surfaces and center during lithium intercalation and de-intercalation, are expected to contribute to the enhanced electrochemical performance of carbon-coated $LiFePO_4$.

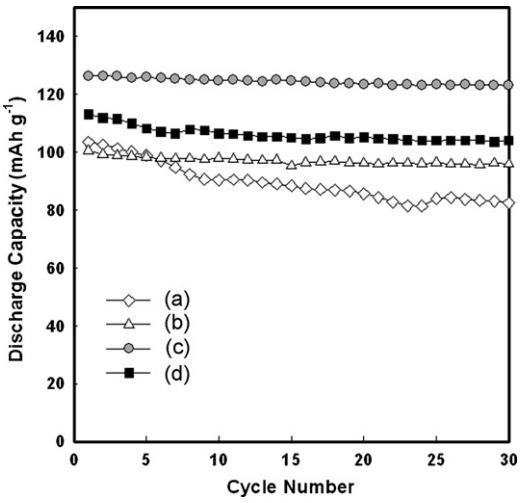

Fig. 5. Cycling performance of $LiFePO_4$-C/SPE/Li cells with different carbon black contents (a) 0 wt.%, (b) 3 wt.%, (c) 5 wt.% and (d) 10 wt.% at a constant current density of 0.1 mA cm^{-2} (cycled between 2.5 and 4.3 V).

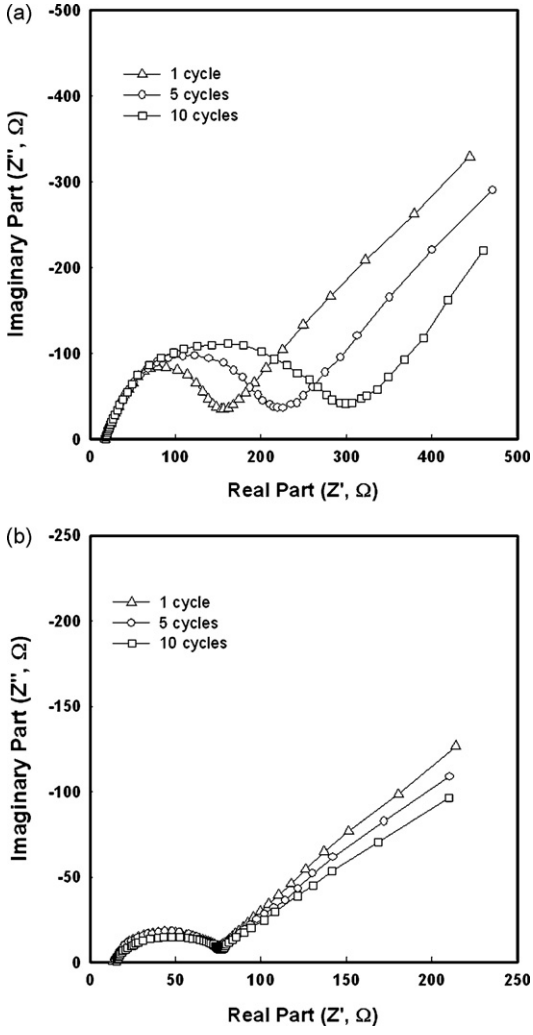

Fig. 6. Impedance spectra of LiFePO4-C/SPE/Li cells with different carbon black contents (a) 0 wt.% and (b) 5 wt.% at a constant current density of 0.1 mA cm^{-2} upon cycling.

3.3. Particle size distribution of $LiFePO_4$-C powders

Particle size distribution of $LiFePO_4$-C powders with different carbon black contents (0, 3, 5 and 10 wt.%) is shown in Fig. 3. As shown from Fig. 3, approximately 72% of $LiFePO_4$ is within 200–300 nm range, approximately 94% of $LiFePO_4$-C with 3 wt.% carbon black is within 150–250 nm range, approximately 62% of $LiFePO_4$-C with 5 wt.% carbon black is within 100–150 nm range, approximately 50% of $LiFePO_4$-C with 10 wt.% carbon black is within 100–150 nm range. It is obvious that the particle size of $LiFePO_4$-C with 5 wt.% carbon black is the smallest.

3.4. Cyclic voltammetry of $LiFePO_4$-C/SPE/Li batteries

Fig. 4 shows cyclic voltammograms of $LiFePO_4$-C/SPE/Li cells with different carbon black contents (0 and 5 wt.%). As shown from Fig. 4a, the oxidation and reduction peak positions for $LiFePO_4$/SPE/Li cell appear at 3.79 and 3.01 V vs. Li/Li^+, respectively; the voltage difference between the oxidation and reduction potential is 0.78 V, and the oxidation and reduction peak positions remove to high potential and low potential upon cycling, respectively. As shown in Fig. 4b, the oxidation and reduction peak positions for $LiFePO_4$-C/SPE/Li cell with 5 wt.% carbon black appear at 3.59 and 3.29 V vs. Li/Li^+, respectively. The voltage difference between oxidation and reduction potential is 0.30 V, and the oxidation and reduction peak positions hardly remove to high potential or low potential, which demonstrates that the electrochemical reaction reversibility of $LiFePO_4$-C/SPE/Li cell with 5 wt.% carbon black is fairly excellent. This indicates that Fe^{2+}/Fe^{3+} redox pairs contribute to the gain and loss of electron in $LiFePO_4$-C (5 wt.%) crystal structures during the lithium insertion/extraction process.

3.5. Cycling performance of $LiFePO_4$-C/SPE/Li cells

Cycling performance of $LiFePO_4$-C/SPE/Li cells with different carbon black contents (0, 3, 5 and 10 wt.%) is shown in Fig. 5. The batteries were cycled between 2.5 and 4.3 V at a current density of 0.1 mA cm^{-2}. As can be seen from Fig. 5, the discharge capacity of $LiFePO_4$/SPE/Li cell is 104 mAh g^{-1} at the first cycle and 86 mAh g^{-1} after 30 cycles, respectively. The initial discharge capacity of $LiFePO_4$-C/SPE/Li cell with 3, 5 and 10 wt.% carbon black is 100, 128 and 114 mAh g^{-1}, respectively. After 30 cycles, the discharge capacity of $LiFePO_4$-C with 3, 5 and 10 wt.% carbon black is 99, 127 and 110 mAh g^{-1}, respectively. It is demonstrated that cycling performance of $LiFePO_4$-C/SPE/Li cells is better than that of $LiFePO_4$/SPE/Li cell and the discharge capacity of $LiFePO_4$-C is the largest when carbon black content is 5 wt.%.

3.6. Impedance spectra of $LiFePO_4$-C/SPE/Li cells

Impedance spectra of $LiFePO_4$-C/SPE/Li cells with different carbon black contents (0 and 5 wt.%) at a constant current density of 0.1 mA cm^{-2} upon cycling are shown in Fig. 6. The batteries were cycled between 2.5 and 4.3 V. It is noted that the ac impedance response of the cell forms a broad semi-circle and a line to the real axis in the lowest frequency range. The inclined line in the lower frequency is attributed to the Warbug impedance, which is associated with lithium ion diffusion in $LiFePO_4$. As can be seen from Fig. 6a, the resistance of $LiFePO_4$/SPE/Li cell is 150 Ω at the first cycle, 210 Ω after 5 cycles, 300 Ω after 10 cycles, respectively. It is obvious that the resistance of $LiFePO_4$/SPE/Li cell increases upon cycling. As can be seen from Fig. 6b, the resistance of $LiFePO_4$-C/SPE/Li cell with 5 wt.% carbon black is 75 Ω at the first cycle, 76 Ω after 5 cycles, 76 Ω after 10 cycles, respectively. It is noted that the resistance of $LiFePO_4$-C/SPE/Li cell with 5 wt.% carbon black hardly changes upon cycling. Therefore, as can be seen from Fig. 5, cycling performance of $LiFePO_4$-C/SPE/Li cell with 5 wt.% carbon is better than that of $LiFePO_4$/SPE/Li cell.

4. Conclusions

Phospho-olivine $LiFePO_4$ cathode materials were successfully prepared by hydrothermal reaction. Carbon black was added to enhance the electrical conductivity of $LiFePO_4$. Lithium polymer cells with $LiFePO_4$-C (0, 3, 5 and 10 wt.%) as cathode materials and 25PVDF-$LiClO_4EC_{10}PC_{10}$ as SPE were evaluated. The charge/discharge results showed that initial discharge capacity of $LiFePO_4$ was 104 mAh g^{-1}. The discharge capacity of $LiFePO_4$-C/SPE/Li cell with 5 wt.% carbon black was 128 mAh g^{-1} at the first cycle and 127 mAh g^{-1} after 30 cycles, respectively. It was demonstrated that cycling performance of $LiFePO_4$-C (3, 5 and 10 wt.%)/SPE/Li cells was better than that of $LiFePO_4$/SPE/Li cells.

Acknowledgement

This research project received supporting funds from the second-stage Brain Korea 21.

References

[1] M. Morcrette, C. Wurm, C. Masquelier, Solid State Sci. 4 (2002) 239–246.
[2] A.S. Anderssona, B. Kalskab, L. Häggströmb, J.O. Thomas, Solid State Ionics 130 (2000) 41–52.
[3] K. Zaghib, K. Striebel, A. Guerfi, J. Shim, M. Armand, M. Gauthier, Electrochim. Acta 50 (2004) 263–270.
[4] A.K. Padhi, K.S. Nanjundaswamy, J.B. Goodenough, J. Electrochem. Soc. 144 (1997) 1188–1194.
[5] A.K. Padhi, K.S. Nanjundaswamy, C. Masquelier, S. Okada, J.B. Goodenough, J. Electrochem. Soc. 144 (1997) 1609–1613.
[6] G. Meligrana, C. Gerbaldi, A. Tuel, S. Bodoardo, N. Penazzi, J. Power Sources 160 (2006) 516–522.
[7] M. Takahashi, S. Tobishima, K. Takei, Y. Sakurai, Solid State Ionics 148 (2002) 283–289.
[8] K. Dokko, S. Koizumi, K. Sharaishi, K. Kanamura, J. Power Sources 165 (2007) 656–659.
[9] S.T. Myung, S. Komaba, N. Hirosaki, H. Yashiro, N. Kumagai, Electrochim. Acta 49 (2004) 4213–4222.
[10] D.-H. Kim, J.-K. Kim, Electrochem. Solid-State Lett. 9 (9) (2006) A439–A442.

[11] G. Arnold, J. Garche, R. Hemmer, S. Ströbele, C. Vogler, M. Wohlfahrt-Mehrens, J. Power Sources 119/121 (2003) 247–251.
[12] S. Franger, F.L. Cras, C. Bourbon, H. Rouault, J. Power Sources 119/121 (2003) 252–257.
[13] H. Huang, S.C. Yin, L.F. Nazar, Electrochem. Solid-State Lett. 4 (2001) A170–A172.
[14] H. Gabrisch, J.D. Wilcox, M.M. Doeff, Electrochem. Solid-State Lett. 9 (2006) A360–A363.
[15] H.T. Chung, S.K. Jang, H.W. Ryu, K.B. Shim, Solid State Commun. 131 (2004) 549–554.
[16] P. Subramanya Herle, B. Ellis, N. Coombs, L.F. Nazar, Nat. Mater. 3 (2004) 147–152.
[17] Y.K. Masuda, M. Nakayama, M. Wakihara, Solid State Ionics 178 (2007) 981–986.
[18] J. Yang, J.J. Xu, J. Electrochem. Soc. 153 (4) (2006) A716–A723.
[19] S. Yang, P.Y. Zavalij, M.S. Whittingham, Electrochem. Commun. 3 (2001) 505–508.
[20] K.S. Park, J.T. Son, H.T. Chung, S.J. Kim, C.H. Lee, H.G. Kim, Electrochem. Commun. 5 (2003) 839–842.
[21] J.-U. Kim, Y.-J. Jo, G.-C. Park, W.-J. Jeong, H.-B. Gu, J. Power Sources 97/98 (2001) 450–453.